Available online at www.sciencedirect.com
ScienceDirect
Biochemical and Biophysical Research Communications 354 (2007) 379–384
BBRC
www.elsevier.com/locate/ybbrc

The diffusive search mechanism of processive myosin class-V motor involves directional steps along actin subunits

Takuya Okada [a,b,c], Hiroto Tanaka [a,c], Atsuko Hikikoshi Iwane [c,d], Kazuo Kitamura [e], Mitsuo Ikebe [f], Toshio Yanagida [a,b,c,d,*]

[a] Formation of Soft Nano-Machines, CREST JST, 1-3, Yamadaoka, Suita, Osaka 565-0871, Japan
[b] Department of Biophysical Engineering, Osaka University, 1-3, Machikaneyama, Toyonaka, Osaka 560-8531, Japan
[c] Laboratories for Nanobiology, Graduate School of Frontier Biosciences, Osaka University, 1-3, Yamadaoka, Suita, Osaka 565-0871, Japan
[d] Department of Physiology and Biosignaling, Graduate School of Medicine, Osaka University, 2-2, Yamadaoka, Suita, Osaka, 565-0871, Japan
[e] Department of Neuroscience, Graduate School of Medicine, Osaka University, 2-2, Yamadaoka, Suita, Osaka, 565-0871, Japan
[f] Department of Physiology, University of Massachusetts Medical School, 55 Lake Avenue North, Worcester, MA 01655-0127, USA

Received 7 December 2006
Available online 8 January 2007

Abstract

It is widely accepted that the vesicle-transporter myosin-V moves processively along F-actin with large steps of ~36 nm using a hand-over-hand mechanism. A key question is how does the rear head of two-headed myosin-V search for the forward actin target in the forward direction. Scanning probe nanometry was used to resolve this underlying search process, which was made possible by attaching the head to a relatively large probe. One-headed myosin-V undergoes directional diffusion with ~5.5 nm substeps to develop an average displacement of ~20 nm, which was independent of the neck length (2IQ and 6IQ motifs). Two-headed myosin-V showed several ~5.5 nm substeps within each processive ~36 nm step. These results suggest that the myosin-V head searches in the forward direction for the actin target using directional diffusion on the actin subunits according to a potential slope created along the actin helix.

Keywords: Myosin-V; Actin filament; 5.5 nm substep; Processive movement; Scanning probe nanometry

Class-V myosin is a processive motor that transports organelles in cells [1,2]. Myosin-V has two heads, each with a long neck [3] (6IQ motifs), and moves along F-actin (actin filament) with large steps of ~36 nm. This step size coincides with an actin half helical pitch [1]. Electron microscopy [4] and single molecule nano-scale imaging (FIONA) [5] have shown that myosin-V walks along the actin helical repeats using a hand-over-hand mechanism. Single molecule polarized fluorescence microscopy [6] and structural studies [7–9] have proposed that the rear head diffuses towards the forward target, with a bias by tilting the long neck. This tilting coupled to a rotation of the front head is based on the crossbridge tilting model [10,11]. The bending rigidity of the neck of myosin-V is ~0.2 pN/nm [12,13] and the displacement of one-headed myosin-V 6IQ is ~24 nm [12,13]. This displacement would not be sufficient to lead the rear head to the forward actin target by tilting the neck fast enough particularly against high loads (2–3 pN). Furthermore, a truncation mutant of myosin-V that has a short neck (1IQ motif), that is, no rigid long neck domain, can move processively with large, ~36 nm steps, the same as that for wild-type myosin-V (6IQ motifs) [14]. These results suggest that another mechanism operates the search mechanism of the rear head.

The diffusive movement of the rear head occurs too fast ($\ll$1 ms) to be detected by optical trapping nanometry [1] and single molecule nano-scale imaging [5]. In this study, we used scanning probe nanometry to resolve the diffusive process of the head, which had been slowed by attaching

* Corresponding author. Fax: +81 6 6879 4634.
E-mail address: yanagida@phys1.med.osaka-u.ac.jp (T. Yanagida).

0006-291X/$ - see front matter © 2006 Elsevier Inc. All rights reserved.
doi:10.1016/j.bbrc.2006.12.200

the head to a relatively large probe [15,16]. We found that one-headed myosin-V underwent directional diffusion with ~5.5 nm substeps to produce an average displacement of ~20 nm, which was independent of the neck size (2IQ and 6IQ motifs). The two-headed myosin-V showed processive ~36 nm steps. Within each of these steps an intermediate step was observed, which has been observed at high loads [17] or in the presence of 2,3-butanedione 2-monoxime [18]. The intermediate step of ~17 nm could be further resolved into several ~5.5 nm substeps. The results strongly indicate that the myosin-V head moves along actin monomers. Based on these results, we propose a mechanism whereby the myosin-V head searches in the forward direction along an actin filament by directional diffusion according to a potential slope along the actin helix.

Materials and methods

To obtain recombinant one-headed myosin-V, SF9 cells were co-infected with two separate viruses expressing human myosin-V heavy chain (2IQ and 6IQ) and calmodulin. To obtain recombinant two-headed myosin-V, mouse myosin-V heavy chain was used [19]. Actin was obtained from rabbit skeletal muscle and purified as described previously [20]. α-actinin was obtained from chicken gizzard and prepared as described previously [21]. Cy5-labeled actin monomers were prepared by conjugating Cy5-maleimide to reactive Cys-374 of actin as described previously [22]. The biotinylated F-actin was prepared as previously described [23]. Biotin-BSA was prepared as previously described [23]. A scanning probe was prepared as previously described [15].

A scanning probe measurement system was constructed based on an inverted fluorescence microscope (IX70, Olympus, Japan) as previously described with some modifications [15]. A blue laser ($\lambda = 488$ nm, Sapphire 488-20-CDRH, Coherent, Japan) was used for measuring the position of the probe. The bright field image of the scanning probe was projected to a split photodiode for nanometer measurements (Fig. 1A). The blue laser was also used to illuminate GFP fused to myosin through objective-type TIRFM by switching the beam path. The fluorescence image was detected by a SIT camera (C2741-08, Hamamatsu Photonics, Japan) with an image intensifier (C8600-03, Hamamatsu Photonics, Japan). A red laser ($\lambda = 632.8$ nm, 05-LHP-928, Melles Griot, USA) was used to illuminate Cy5-labeled actin bundles through an objective-type TIRFM. For myosin-V HMM, a previously described system was used [15].

Fluorescence images of GFP fused to myosin acquired at 33.3 ms intervals were stored on a PC with a DAQ board (PCI-1409, National Instruments, USA) and analyzed using Labview (National Instruments, USA) image analysis system. The displacement of the scanning probe was recorded at 24 kHz sampling rate by a DAT recorder (LX10, TEAC, Japan) and analyzed as previously described [15]. The change in stiffness from low stiffness (0.01–0.07 pN/nm) to high stiffness (0.3–1.0 pN/nm) was considered an indicator of the interaction between the actin filament and myosin head [24]. All pairwise distance analysis was used to analyze the rising phases [25,26].

Results

The captured myosin heads were visualized using the fluorescence of fused GFP detected by total internal reflection fluorescence microscopy (TIRFM) [27,28] in conjunction with a scanning probe microscope (Fig. 1A). The single one-headed myosin-V captured onto the probe was brought into contact with actin bundles formed by α-actinin fixed on a glass surface. The displacements were determined by measuring the deflection of the needle with a split photodiode with nanometer accuracy (Fig. 1A). For two-headed myosin-V, we confirmed that single two-headed myosin-V molecules were sufficient to move the probe using conventional analysis [29].

Fig. 1B shows typical traces of displacements (upper green traces) and their rising phases on an expanded time scale (lower blue traces), produced by a one-headed myosin-V with a short neck (2IQ motifs) (B) or a long neck (6IQ motifs) (C), all in the presence of 1 μM ATP at 15 °C. One-headed myosin-V showed non-processive displacements. Displacements did not take place abruptly but instead developed in a stepwise fashion. In order to resolve the displacements, we took all pairwise distance of the rising phase of each displacement and its power spectrum (Supplementary Fig. 1). The pairwise distances and their power spectra for 169 (63%) out of 267 observed displacements by one-headed myosin-V with 2IQ in 7 different experiments at 15 and 20 °C showed peaks corresponding to ~5.5 nm and/or ~11 nm substeps. Fig. 2A shows a histogram of pairwise distances averaged for the rising phases of these 169 displacements. The power spectrum showed a clear peak corresponding to ~5.5 nm substep, indicating that the rising phases of displacements included ~5.5 nm. The substeps of ~11 nm most likely correspond to $2 \times$ ~5.5 nm substeps occurring within the temporal resolution of the measurement system. However, the remaining 98 (37%) displacements showed no clear substeps in their rising phases. The present measurement system was able to resolve the ~5.5 nm substeps whose dwell times were >~1 ms ($\tau = (2\pi fc)^{-1}$, where f_c is the corner frequency of the needle, ~200 Hz). Therefore, the most likely explanation for the absence of 5.5 nm substeps is that they took place within the time and spatial resolution of the measurement system (Supplementary Fig. 2). Those exhibiting no clear steps were consistent with the results of a computer simulation on the effect of noise on the detection of 5.5 nm steps. For negative controls, we performed the pairwise distance and power spectrum analyses for three periods during which rising phases included 5.5 and/or 11 nm steps: in between displacement events, during plateaus, and during the falling phases of displacements. Neither pairwise distance nor power spectrum in these three groups had 5.5 or 11 nm steps. The data are shown in supplementary materials (Supplementary Fig. 3A–C).

Substeps were also observed for one-headed constructs with a long (6IQ) neck. The pairwise analysis indicated that 46 (35%) and 37 (28%) out of observed 130 displacements (2 different experiments) at 15 °C included ~5.5 nm and ~11 nm substeps, respectively. For the remaining 47 (37%) displacements, substeps were not clear. The thermal noise created by the vibration of the needle resulting from the large compliance of the long neck was larger than that for the construct with a short (2IQ) neck, so in the pairwise distance and power spectrum averaged for all displace-

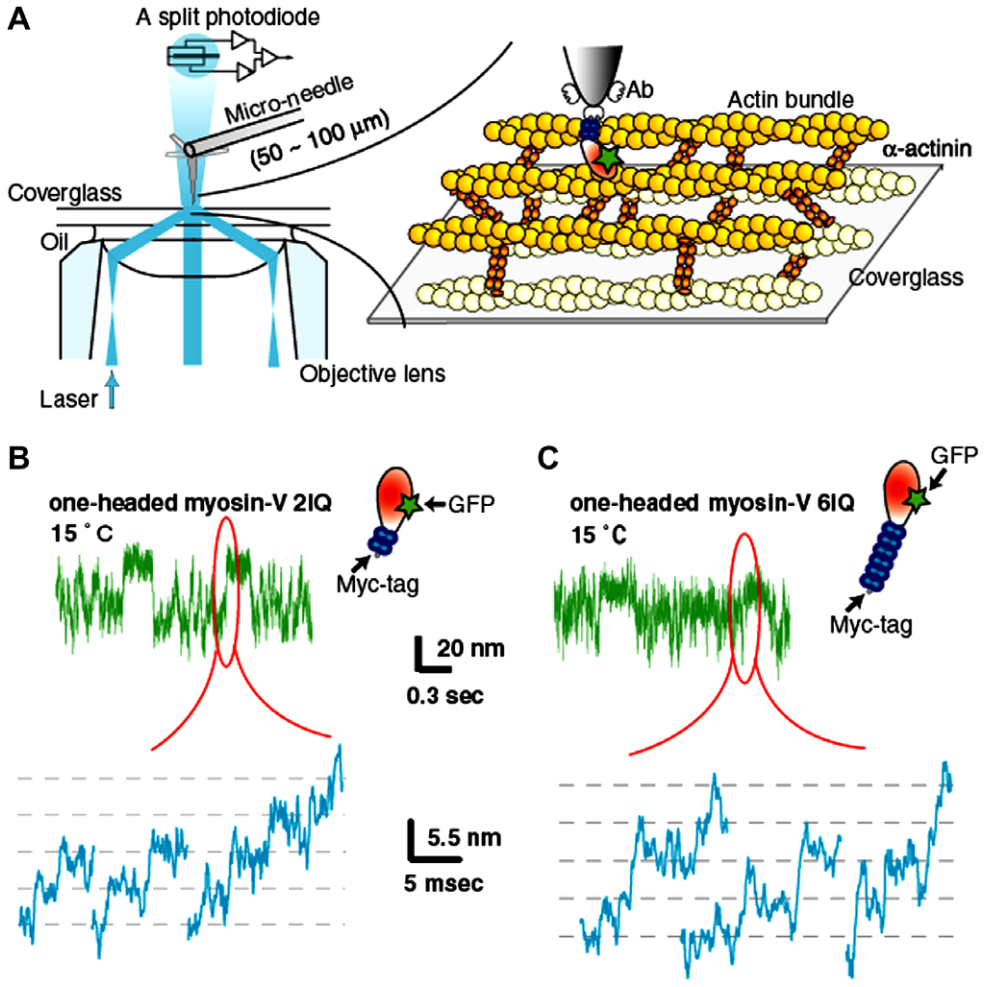

Fig. 1. Schematic drawing of the experimental apparatus and substeps in the rising phases of displacements. (A) Schematic drawing of the measurement system. A scanning probe nanometry system originally made to resolve the detailed processes of the displacement of myosin II [15,16] was used with some modifications. In this measurement, a blue laser was used for single molecule GFP imaging in an objective-type TIRFM and for bright field image of a scanning probe on a split photodiode for nanometer measurements. A single myosin molecule, which had been fused to GFP, was specifically attached to the tip of a scanning probe through myc tag via c-Myc monoclonal antibody (Ab). The one-headed myosin-V was rigidly attached to a reasonably large scanning probe, so it was assumed to stably interact with an actin filament without diffusing away. (B) Typical recordings of the time courses of displacements (upper) and rising phases of displacements on an expanded time scale (lower) by a one-headed myosin-V 2IQ. (C) Typical recordings of the time courses of displacements (upper) and rising phases of displacements on an expanded time scale (lower) by a one-headed myosin-V 6IQ. [ATP] = 1 μM and $T = 15$ °C.

ments exhibiting ~5.5 nm and/or ~11 nm substeps, the peak corresponding to 5.5 nm substeps was damped. Therefore we analysed these separately. The power spectrum of all pairwise distances averaged for the 46 displacements showed a peak corresponding to ~5.5 nm substeps (Fig. 2B) and that averaged for the 37 displacements showed a peak corresponding to ~11 nm substeps.

The number of ~5.5 nm substeps per displacement for one-headed myosin-V 2IQ was between 1 and 7 with a mean of 3.6 ± 0.2 steps (Fig. 2C), which was similar to that of one-headed myosin-V 6IQ (3.8 ± 0.2 steps) (Fig. 2D).

The mechanical kinetics of displacements and ~5.5 nm substeps by one-headed myosin-V 2IQ at different ATP concentrations at 20 °C were analyzed. The mean durations of displacements were 0.28 and 1.3 s at 1 and 0.2 mM ATP, respectively. These durations give the second order association constant of ATP for actin–myosin complexes of ~3.4 $\mu M^{-1}s^{-1}$. This value was slightly larger than those obtained by a previous study for one-headed myosin-V with a short neck (1IQ) (~2.0 $\mu M^{-1}\ s^{-1}$) [30]. The ATP binding to an actomyosin-V complex is strain dependent [12]. Therefore, the strain exerted on myosin-V head attached to a large scanning probe would be different. This result indicates that each displacement corresponds to a single ATPase cycle by a single myosin head. This is in agreement with the fluorescence observations of GFP fused to the head of the probe. On the other hand, the mean dwell times for ~5.5 nm substeps observed in the rising phases of displacements were constant, independent of the concentration of ATP. Furthermore, the dwell times (2–3 ms) of the ~5.5 nm substeps were >100-fold shorter than the ATP turnover time at 1 μM ATP. Thus, these

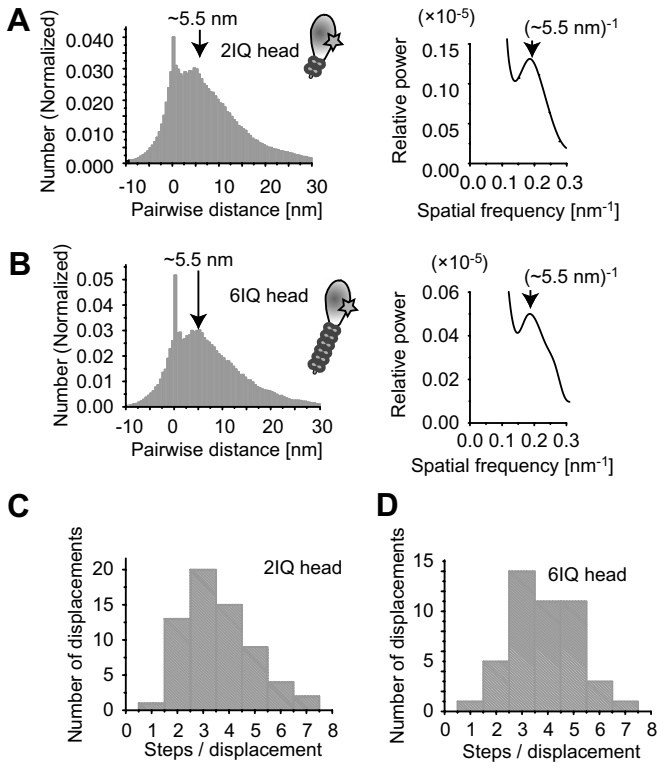

Fig. 2. Analyses of substeps. (A) A histogram of pairwise distance for all data points of the rising phases of observed displacements primarily constituted ~5.5 nm and/or ~11 nm substeps (169 out of 268 displacements from 7 different experiments) by one-headed myosin-V 2IQ (left) at 15 and 20 °C and the power spectrum of the histogram of all measurements for pairwise distance (right) (See text for selection). (B) A histogram of all pairwise distance averaged for displacements primarily constituting substeps of ~5.5 nm (46 displacements out of 130 displacements from 2 different experiments) by one-headed myosin-V 6IQ (left) and its power spectrum (right) at 15 °C. Histograms of the number of ~5.5 nm substeps per displacement for one-headed myosin-V 2IQ (C) and 6IQ (D). [ATP] = 1 μM.

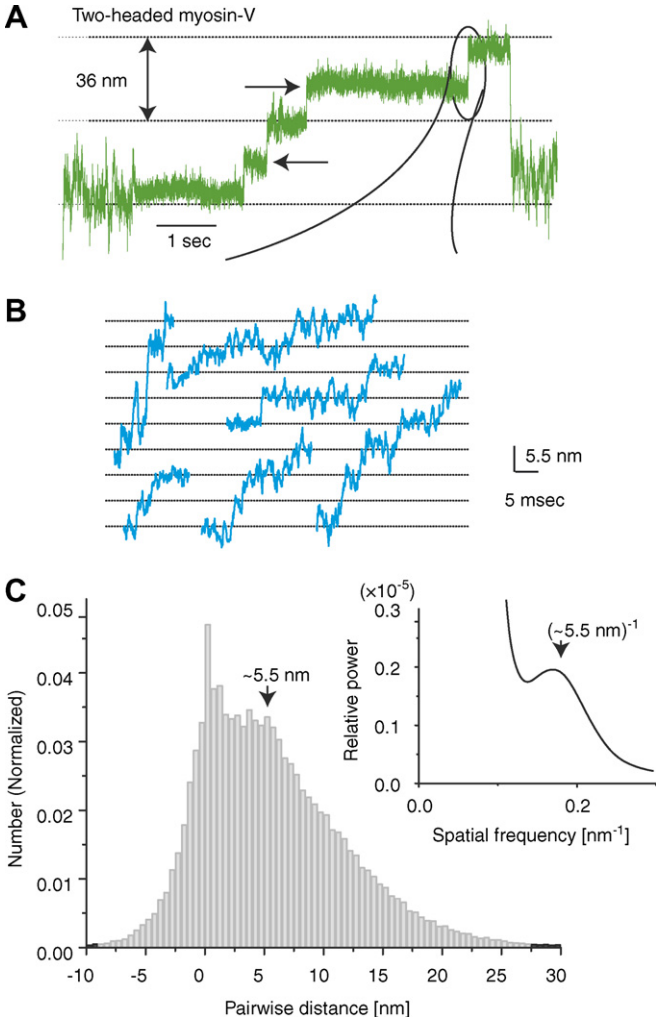

Fig. 3. (A) Typical recordings of the time courses of displacements by a two-headed myosin-V. Arrows indicate intermediate steps (see text). (B) Time courses of the rising phases of displacements by a two-headed myosin-V on an expanded time scale. [ATP] = 2 μM or 2 mM and $T = 20$ °C. (C) A histogram of all pairwise distances averaged for 46 displacements (3 different experiments) primarily constituted ~5.5 nm substeps and/or ~11 nm and the power spectrum (insertion).

results indicate that the observed multiple ~5.5 nm substeps take place within a single ATP hydrolysis event caused by a single myosin head.

A two-headed myosin-V showed processive movement with ~34 nm steps (Fig. 3A) as previously observed by optical trapping nanometry [1,17,18]. Furthermore an intermediate step (~17 nm) within each 34 nm step was observed (Fig. 3A, arrow). Such intermediate steps have been previously observed using optical trapping nanometry at high loads [17] or in the presence of 2,3-butanedione monoxime [18]. In this experiment, the intermediate step was clearly observed even at low loads. It is likely that the intermediate step was also slowed by attaching the two-headed myosin-V to a large scanning probe. Fig. 3B shows the rising phases of the intermediate steps on an expanded time scale. The substeps of ~5.5 nm could be clearly observed. The number of ~5.5 nm substeps within each intermediate step varied from between 1 and 6 with a mean number of ~3. Fig. 3C shows a histogram of all the pairwise distance of the rising phases and the power spectrum (insertion) averaged for 46 displacements (3 different experiments). Clear peaks were observed at the positions corresponding to ~5.5 nm substeps. ~5.5 nm substeps were observed for both the first and second intermediate steps. This is probably because the rear head interacts with actin in the backward actin helix region (see Discussion). The size of substeps (~5.5 nm) observed near the maximum force was similar to that at low loads, indicating that the size of substeps was independent of load.

Discussion

The total number of ~5.5 nm substeps per displacement was between 1 and 7 with a mean value of 3–4 steps (Figs. 2C, D and 3B). The substepsize (~5.5 nm) coincides with the distance between adjacent actin subunits and the

maximum stepping distance (~5.5 nm × 7) was approximately half the helical pitch of an actin filament (36 nm). Furthermore, the size of the substeps (~5.5 nm) was constant and independent of the myosin head neck domain size and the load. Thus, the results suggest that the myosin head undergoes directional steps on actin subunits according to a potential slope along the half helical pitch of an actin filament (Fig. 4A). The potential slope may be due to conformational changes in the actin filament [31,32]. The binding sites for a myosin head rotate along the F-actin helix. Therefore, when the myosin head fixed on the probe tip is brought into contact with an actin filament fixed on a glass surface, the steric compatibility between the orientation of the actin binding sites and the myosin head changes along the F-actin helix [14]. Thus, this steric compatibility should make a potential slope along the half helix of F-actin as previously suggested by Veigel et al. [33].

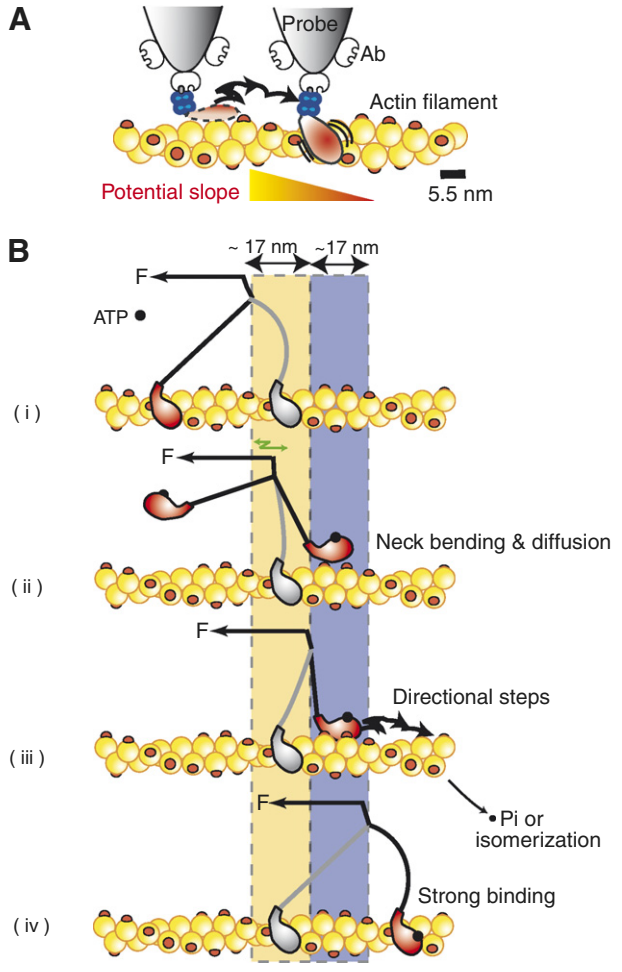

Fig. 4. Hopping model for myosin-V stepping. (A) Potential slope along the actin helix. The potential slope is generated by the steric compatibility between the orientations of the actin and the myosin head (see text for detail). (B) The hopping model for myosin-V stepping. The rear head searches for the actin target in the forward direction by a hopping movement on the actin subunits according to a potential slope along the actin helix (see text for detail). Black closed circle, ATP or ADP-Pi. F = Force. Yellow of ~17 nm indicate displacements by the neck bending and its diffusion. Gray bands of ~17 nm indicate directional steps on actin monomers according to the potential slope along the actin helix.

Based on these results, we propose a hopping model for two-headed myosin-V (Fig. 4B). ATP favorably binds to the rear head because of an intramolecular strain through the bending of the neck [12] (Fig. 4B (i)). The rear head detaches from actin and undergoes Brownian motion back and forth along the backward actin helix region, probably interacting with actin in the weak binding state because ~5.5 nm substeps were observed when trailing the front head (Fig. 4B (ii)). When the rear head moves beyond the front head, it undergoes directional hopping over approximately 3 actin subunits (~17 nm) according to a potential slope along the actin helix (Fig. 4B (iii)). This results in the movement of the stalk of myosin-V by ~16.5 nm (3× 5.5 nm). When the rear head reaches the bottom of the potential i.e., the forward target, the negative strain is exerted on the neck domain of head and the release of Pi from the myosin head or isomerization of the myosin head is accelerated to form strong binding [34–36] (Fig. 4B (iv)). Thus, the myosin-V walks along the F-actin with ~36 nm steps.

Acknowledgments

This work was supported by a CREST JST. We are grateful to Drs. O. Ohara and H. Yamakawa for providing cDNA fragments of human myosin-V; Ms. T. Mimuro for generating the human Myosin-V construct; Drs. Y. Ishii, P. Karagiannis, M. Zulliger and J. West for critically reading the manuscript and helpful discussions; colleagues of the Yanagida Laboratory at the Single Molecule Processes Project, Formation of soft nano-machines, and Osaka University for discussion.

Appendix A. Supplementary data

Supplementary data associated with this article can be found, in the online version, at doi:10.1016/j.bbrc.2006.12.200.

References

[1] A.D. Mehta, R.S. Rock, M. Rief, J.A. Spudich, M.S. Mooseker, R.D. Cheney, Myosin-V is a processive actin-based motor, Nature 400 (1999) 590–593.
[2] S.L. Reck-Peterson, D.W. Provance Jr., M.S. Mooseker, J.A. Mercer, Class V myosins, Biochem. Biophys. Acta 1496 (2000) 36–51.
[3] R.E. Cheney, M.K. Oshea, J.E. Heuser, M.V. Chelho, J.S. Wolenski, E.M. Espreafico, P. Forscher, R.E. Larson, M.S. Mooseker, Brain myosin-V is a two-headed unconventional myosin with motor activity, Cell 75 (1993) 13–23.
[4] M.L. Walker, S. A Burgess, J.R. Sellers, F. Wang, J.A. Hammer III, J. Trinick, P.J. Knight, Two-headed binding of a processive myosin to F-actin, Nature 405 (2000) 804–807.
[5] A. Yildiz, J.N. Forkey, S.A. McKinney, T. Ha, Y.E. Goldman, P.R. Selvin, Myosin-V walks hand over hand: single fluorophore imaging with 1.5 nm localization, Science 300 (2003) 2061–2065.

[6] J.N. Forkey, M.E. Quinlan, M.A. Shaw, J.E. Corrie, Y.E. Goldman, Three dimensional structural dynamics of myosin-V by single-molecule fluorescence polarization, Nature 422 (2003) 399–404.
[7] P.-D. Coureux, A.L. Wells, J. Menetrey, C.M. Yengo, C.A. Morris, H. L Sweeney, A. Houdusse, A structural state of the myosin V motor without bound nucleotide, Nature 425 (2003) 419–423.
[8] P.-D. Coureux, H.L. Sweeney, A. Houdusse, Three myosin V structures delineate essential features of chemo-mechanical transduction, EMBO J. 23 (2004) 4527–4537.
[9] N. Volkmann, H. Liu, L. Hazelwood, E.B. Krementsova, S. Lowey, K.M. Trybus, D. Hanein, The structural basis of myosin V processive movement as revealed by electron cryomicroscopy, Mol. Cell 19 (2005) 595–605.
[10] H.E. Huxley, The mechanism of muscular contraction, Science 164 (1969) 1355–1366.
[11] A.F. Huxley, R.M. Simmons, Proposed mechanism of force generation in striated muscle, Nature 233 (1971) 533–538.
[12] C. Veigel, S. Schmitz, F. Wang, J.R. Sellers, Load-dependent kinetics of myosin-V can explain its high processivity, Nat. Cell Biol. 7 (2005) 861–869.
[13] T.J. Purcell, C. Morris, H.L. Sweeney, J.A. Spudich, Role of the lever arm in the processive stepping of myosin V, Proc. Nat. Acad. Sci. USA 99 (2002) 14159–14164.
[14] H. Tanaka, K. Homma, A.H. Iwane, E. Katayama, R. Ikebe, J. Saito, T. Yanagida, M. Ikebe, The motor domain determines the large step of myosin-V, Nature 415 (2002) 192–195.
[15] K. Kitamura, M. Tokunaga, A.H. Iwane, T. Yanagida, A single myosin head moves along an actin filament with regular steps of 5.3 nanometres, Nature 397 (1999) 129–134.
[16] K. Kitamura, M. Tokunaga, S. Esaki, A.H. Iwane, T. Yanagida, Mechanism of muscle contraction based on stochastic properties of single actomyosin motors observed in vitro, Biophysics 1 (2005) 1–19. http://www.biophys.jp/.
[17] M. Rief, R.S. Rock, A.D. Mehta, M.S. Mooseker, R.D. Cheney, J.A. Spudich, Myosin-V stepping kinetics: A molecular model for processivity, Proc. Natl. Acad. Sci. USA 97 (2000) 9482–9486.
[18] S. Uemura, H. Higuchi, A.O. Olivares, E.M. De La Cruz, S. Ishiwata, Mechanochemical coupling of two substeps in a single myosin V motor, Nat. Struct. Biol. 11 (2004) 833–877.
[19] K. Homma, J. Saito, R. Ikebe, M. Ikebe, Ca^{2+}-dependent regulation of the motor activity of myosin-V, J. Biol. Chem. 275 (2000) 34766–34771.
[20] J.A. Spudich, S. Watt, The regulation of rabbit skeletal muscle contraction. I. Biochemical studies of the interaction of the tropomyosin–troponin complex with actin and the proteolytic fragments of myosin, J. Biol. Chem. 246 (1971) 4866–4871.
[21] S.W. Craig, C.L. Lancashire, J.A. Cooper, Preparation of smooth muscle α-actinin, Methods Enzymol. 85 (1982) 316–321.
[22] A. Ishijima, H. Kojima, T. Funatsu, M. Tokunaga, H. Higuchi, H. Tanaka, T. Yanagida, Simultaneous observation of individual ATPase and mechanical events by a single myosin molecule during interaction with actin, Cell 92 (1998) 161–171.
[23] T. Sakamoto, I. Amitani, E. Yokota, T. Ando, Direct observation of processive movement by individual myosin V molecules, Biochem. Biophys. Res. Commun. 272 (2000) 586–590.
[24] J.E. Molloy, J.E. Burns, J. Kendrick-Jones, R.T. Tregear, D.C.S. White, Movement and force produced by a single myosin head, Nature 378 (1995) 209–212.
[25] S.C. Kuo, J. Gelles, E. Steuer, M.P. Sheetz, A model for kinesin movement from nanometer-level movements of kinesin and cytoplasmic dynein and force measurements, J. Cell Sci. 14 (1991) 135–138.
[26] K. Svoboda, C.F. Schmidt, B.J. Schnapp, S.M. Block, Direct observation of kinesin stepping by optical trapping interferometry, Nature 365 (1993) 721–727.
[27] T. Funatsu, Y. Harada, M. Tokunaga, K. Saito, T. Yanagida, Imaging of single fluorescent molecules and individual ATP turnovers by single myosin molecules in aqueous solution, Nature 374 (1995) 555–559.
[28] M. Tokunaga, K. Kitamura, K. Saito, A.H. Iwane, T. Yanagida, Single molecule imaging of fluorophores and enzymatic reactions achieved by objective-type total internal reflection fluorescence microscopy, Biochem. Biophys. Res. Commun. 235 (1997) 47–53.
[29] K. Svoboda, S.M. Block, Force and velocity measured for single kinesin molecules, Cell 77 (1994) 773–784.
[30] T.J. Purcell, H.L. Sweeney, J.A. Spudich, A force-dependent state controls the coordination of processive myosin V, Proc. Natl. Acad. Sci. USA 102 (2005) 13873–13878.
[31] T. Yanagida, M. Nakase, K. Nishiyama, F. Oosawa, Direct observation of motion of single F-actin filaments in the presence of myosin, Nature 307 (1984) 58–60.
[32] Md.S.P. Siddique, G. Mogami, T. Miyazaki, E. Katayama, T.Q.P. Ueda, M. Suzuki, Cooperative structural change of actin filaments interacting with activated myosin motor domain, detected with copolymers of pyrene-labeled actin and acto-S1 chimera protein, Biochem. Biophys. Res. Commun. 337 (2005) 1185–1191.
[33] C. Veigel, F. Wang, M.L. Bartoo, J.R. Sellers, J.E. Molloy, The gated gait of the processive molecular motor myosin-V, Nat. Cell Biol. 4 (2002) 59–65.
[34] T. Yanagida, S. Esaki, A.H. Iwane, Y. Inoue, A. Ishijima, K. Kitamura, H. Tanaka, M. Tokunaga, Single-motor mechanics and models of the myosin motor, Philos. Trans. R. Soc. Lond. B. Biol. Sci. 355 (2000) 441–447.
[35] T.M. Watanabe, H. Tanaka, A.H. Iwane, S. Maki-Yonekura, K. Homma, A. Inoue, R. Ikebe, T. Yanagida, M. Ikebe, A one-headed class V myosin molecule develops multiple (≈32-nm) steps successively, Proc. Natl. Acad. Sci. USA 101 (2004) 9630–9635.
[36] M. Iwaki, H. Tanaka, A.H. Iwane, E. Katayama, M. Ikebe, T. Yanagida, Cargo binding makes a single-headed myosin-VI move processively, Biophys. J. 90 (2006) 3643–3652.